GEOPHYSICAL RESEARCH LETTERS, VOL. 26, NO.3, PAGES 409-412, FEBRUARY 1, 1999

A quantitative test of the self-organization hypothesis of the magnetopause Kelvin-Helmholtz instability as an inverse problem

Akira Miura

Department of Earth and Planetary Physics, University of Tokyo, Tokyo, Japan

Abstract. The self-organization hypothesis of the magnetopause Kelvin-Helmholtz (K-H) instability is tested against observations by two-dimensional (2-D) magnetohydrodynamic (MHD) simulations for two different initial seed perturbations. The linear relationships are obtained by the simulations between the period of the magnetopause oscillation caused by the K-H instability and the distance along the magnetopause from the subsolar point. The comparison of the linear relationships with that obtained from reported observations of the magnetopause oscillations gives a reasonable thickness of the velocity shear layer near the subsolar point of 1570km-3010km and a reasonable average magnetosheath flow speed along the magnetopause of 399km/sec-766km/sec. This suggests that the self-organization of the magnetopause K-H instability, i.e., the successive pairings of vortices, really occurs along the magnetopause. The present comparison provides a useful method to determine the thickness of the velocity shear layer near the subsolar point as an inverse problem.

Introduction

It has recently been demonstrated by 2-D MHD simulations that successive pairings of vortices occurring in the nonlinear stage of the K-H instability is a self-organization process [*Miura*, 1998]. This suggests that small-scale vortices excited by the instability near the subsolar magnetopause evolve into global-scale vortices in the tail of the magnetosphere.

In the temporal evolution of the K-H instability the wavelength of the dominant mode increases with time due to the pairing of vortices [*Belmont and Chanteur*, 1989; *Miura*, 1997, 1998]. In the spatial development of the instability the wavelength of the magnetopause oscillation caused by the instability increases with the distance along the magnetopause [*Wu*, 1986; *Manuel and Samson*, 1993]. *Chen et al.* [1993] assumed that an observed wavelength of the magnetopause oscillation (~$15R_E$) was represented by the wavelength of the linearly fastest growing mode of the K-H instability. *Belmont and Chanteur* [1989], however, suggested that the K-H instability at the magnetopause must have experienced the inverse cascade in order to be able to explain a long wavelength of the dominant mode of the instability at the magnetopause, which is much larger than the wavelength of the linearly fastest growing mode. Since the thickness of the velocity shear layer increases in the nonlinear evolution of the instability, a self-consistent nonlinear approach is necessary to explain the increase of the dominant wavelength of the K-H instability in the nonlinear stage.

Paper number 1998GL900300.
0094-8276/99/1998GL900300$05.00

The purpose of this paper is to quantify the pairings of vortices in the nonlinear stage of the K-H instability based on simulations and to compare the results with observations of the magnetopause oscillations in order to obtain the thickness of the velocity shear layer near the subsolar point and the average magnetosheath flow speed along the magnetopause. This is a typical approach of an inverse problem, i.e., to obtain those two unknown parameters of the nonlinear partial differential equations from the solution, i.e., the period of the magnetopause oscillation caused by the K-H instability. Although the thickness of the velocity shear layer at the magnetopause has never been measured, it is an important parameter to investigate the magnetopause structure.

Simulation Results

A 2-D MHD simulation of the K-H instability is performed for an initial velocity profile of $v_{0y}(x)=(V_0/2)[1-\tanh(x/a)]$ and for a convective fast mode Mach number of 0.35. The initial uniform magnetic field is perpendicular to the simulation plane (x-y plane). This corresponds to the case where the magnetosheath magnetic field is due north and the magnetopause is most susceptible to the K-H instability [*Miura*, 1995a, 1995b]. Time t is normalized by $2a/V_0$, where 2a is the initial thickness of the velocity shear layer and V_0 is the magnetosheath flow speed, which is assumed constant. The length of the periodic simulation box in the y-direction is equal to 8 times as long as the wavelength of the linearly fastest growing mode (λ_{FGM}=15.7a). In *Miura* [1998] a coherent perturbation, which was a sum of the linearly fastest growing mode and its subharmonics, was given as an initial seed perturbation with the peak amplitude of v_x equal to $0.005V_0$ and the temporal evolution of the instability was investigated. In the real spatial evolution of the instability along the magnetopause the initial seed perturbation should be considered as a seed perturbation near the subsolar point. Since the perturbation near the subsolar point is more likely to be disordered, a random seed perturbation with its peak amplitude of v_x equal to $0.005V_0$ is given as an initial seed perturbation in the present run.

Figures 1(a) and (c) show contours of vorticity at T=60 and T=600, where $T=tV_0/(2a)$. At T=60 eight vortices are observed as predicted by the linear theory, but as a consequence of successive pairings of vortices, a large isolated vortex is formed inside the simulation region at T=600. Figures 1(b) and (d) show electric current vectors at T=60 and T=600. It is seen in these panels that an eddy current is associated with each vortex. The eddy current appears because of the compressiblity, which compresses and rarefies the plasma and the magnetic field in the present 2-D configuration, where the plasma motion occurs in a plane perpendicular to the magnetic field, and it is mainly due to the inertia current [*Miura*, 1997, 1998].

In order to investigate the evolution of each Fourier harmonic, the kinetic energy integrated along the x-direction was Fourier

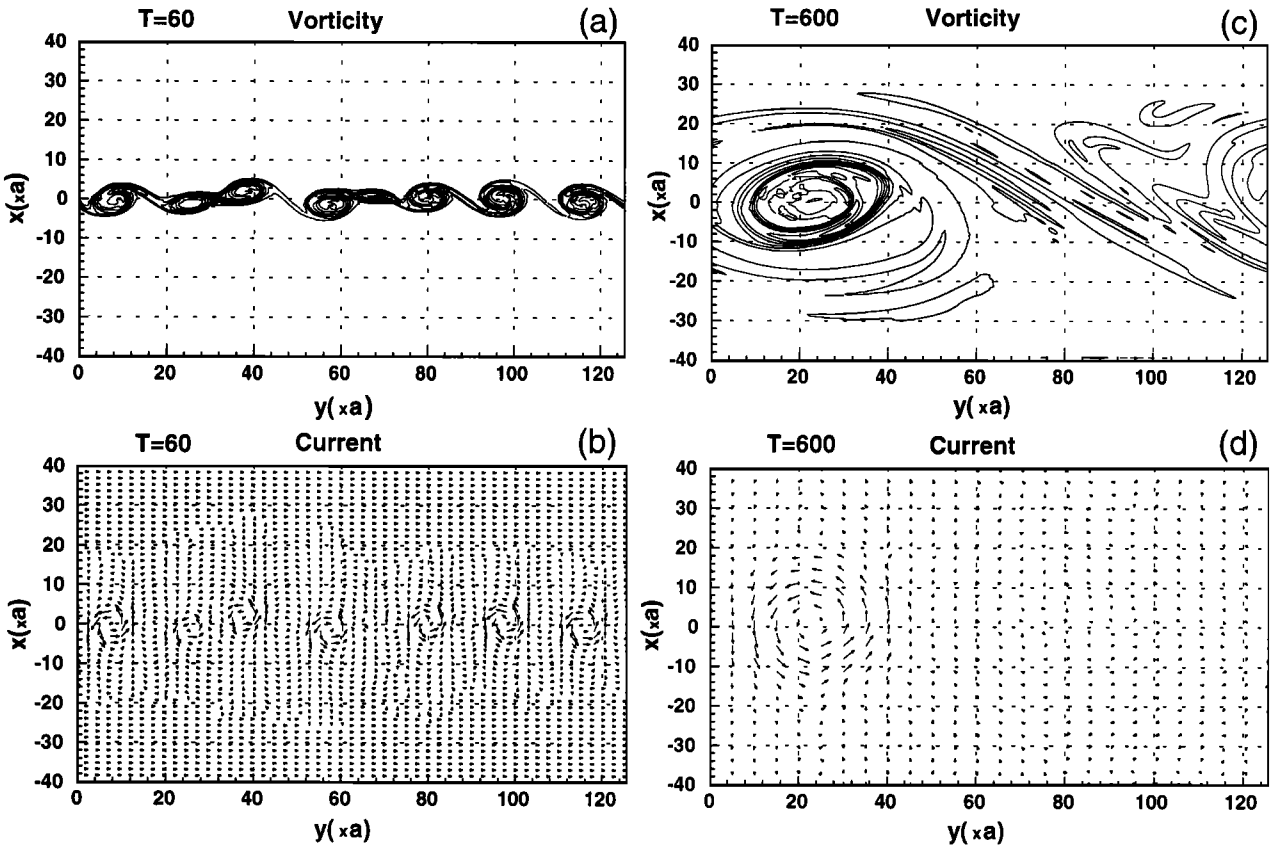

Figure 1. (a) Contours of the vorticity at T=60. (b) Electric current vectors at T=60. (c) Contours of the vorticity at T=600. (d) Electric current vectors at T=600.

analyzed. Figure 2 shows the temporal evolution of the square amplitudes of the 5 Fourier subharmonics with the wavenumbers in the y-direction k/k_{FGM}=1/8, 1/4, 3/8, 1/2, 1, where k_{FGM} $=2\pi/\lambda_{FGM}$. All square amplitudes are normalized by $2ap_0$, where p_0 is the initial uniform pressure. The fastest growing mode with $k= k_{FGM}$ grows fastest in the initial stage, but it quickly saturates with a small amplitude. At the final stage the longest wavelength mode with $k= k_{FGM}/8$ dominates.

Figure 3 shows the plot of the wavelength λ of each subharmonic normalized by λ_{FGM} as a function of time t, when the subharmonic has the peak amplitude. For the fastest growing mode, however, the time t, when the fastest growing mode has an initial peak amplitude and when it dominates the other modes, is used for plotting. It is seen that an almost linear relationship holds between λ and t. A best fit (linear regression line) to the data is represented by the solid line in this figure, which is expressed as

$$\lambda/\lambda_{FGM}=AtV_t/(2a)+B \qquad (1)$$

where A=0.0384 and B=-1.51.

Figure 4 shows a λ vs. t relation for the simulation run, in which the initial seed perturbation was coherent [*Miura*, 1998]. The linear relationship (1) also holds in this case with A=0.02 and B=0.737.

A Method of Determining the Thickness of the Velocity Shear Layer near the Subsolar Point and the Average Flow Speed in the Magnetosheath

Since the time t, when the amplitude of the linearly fastest growing mode is peaked, depends on the amplitude and the phase of the initial seed perturbation, let us assume for simplicity that t=0 is the time when the fastest growing mode takes an initial peak value. Then the linear equation (1) is transformed to

$$\lambda/\lambda_{FGM}=AtV_t/(2a)+1 \qquad (2)$$

Since the present simulation is performed for a homogeneous velocity shear layer, the phase velocity of the unstable wave in the magnetospheric inertial frame is given by $V_t/2$ [*Miura and Pritchett*, 1982; *Miura*, 1997]. Since the vortex moves with the phase velocity of the unstable wave in this frame, the distance L_S from the subsolar point to the location of the vortex traveling

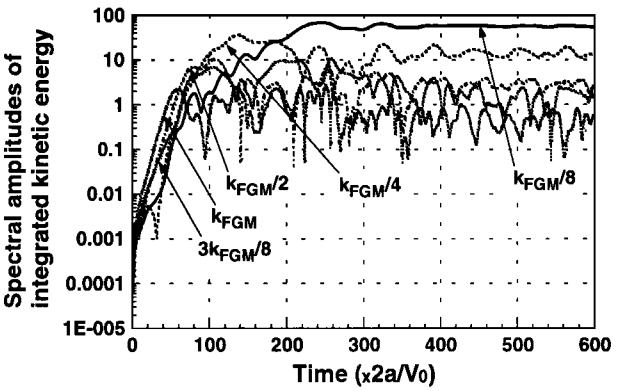

Figure 2. Temporal evolution of the square amplitudes of the Fourier harmonics of the integrated kinetic energy with the wavenumbers in the y-direction k/k_{FGM}=1/8, 1/4, 3/8, 1/2, 1, where k_{FGM} $=2\pi/\lambda_{FGM}$, for the simulation run with a random initial seed perturbation.

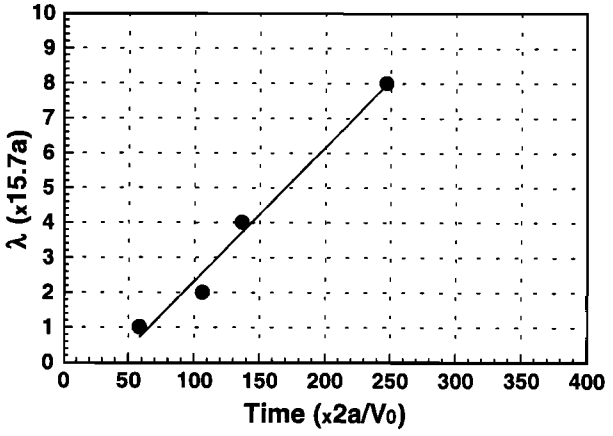

Figure 3. The wavelength of each subharmonic normalized by λ_{FGM} as a function of time t, when the subharmonic has the peak amplitude, for the simulation run with a random initial seed perturbation. The solid line is a regression line.

along the magnetopause is given by $V_0 t/2$. The period τ of the magnetopause oscillation induced by the passage of the vortex is given by $\tau = \lambda/(V_0/2)$. By using $L_S = V_0 t/2$ and $\tau = 2\lambda / V_0$ the formulae (2) can be transformed to

$$\tau = 2\lambda_{FGM} A L_S/(aV_0) + 2\lambda_{FGM}/V_0 \quad (3)$$

This gives a formula based on the simulation results, which gives τ as a function of the distance L_S from the subsolar point along the magnetopause. On the other hand, it is known that the observed period of the magnetopause oscillation increases with the distance from the subsolar point. Let us assume that a linear relationship holds between the observed period τ of the magnetopause oscillation at the distance L_S from the subsolar point along the magnetopause and L_S. We can express this linear relationship based on the observation by

$$\tau = CL_S/R_E + D \quad (4)$$

where R_E=6370km is the earth's radius. By equating equation (3) with equation (4) we obtain the thickness 2a of the velocity shear layer near the subsolar point and the average speed V_0 of the magnetosheath flow along the magnetopause as follows

$$2a = 2ADR_E/C \quad (5)$$

$$V_0 = 2\lambda_{FGM}/D = 15.7 \times 2a/D \quad (6)$$

Comparison of Simulation Results with Observations

Figure 5 is a summary of reported observations showing the oscillation period τ of the magnetopause as a function of the distance L_S from the subsolar point along the magnetopause. The data points in Figure 5 from the left are due to *Williams* [1979], *Kokubun et al.* [1994], *Lepping and Burlaga* [1979], *Seon et al.* [1995], and *Chen et al.* [1993]. Except *Seon et al.* [1995] oscillation periods used in Figure 5 were given in their papers. Although *Seon et al.* [1995] did not calculate the period of the magnetopause oscillation, the period used in Figure 5 was obtained by noting that there were 6 magnetopause crossings between 1400UT and 1500UT in their plate 3, which gave an oscillation period of 600sec. The oscillations of *Chen et al.* [1993], *Kokubun et al.* [1994], and *Seon et al.* [1995] occurred when the magnetosheath magnetic fields were northward or strongly northward and thus the magnetopause was most succeptible to the K-H instability [*Miura*, 1995a, 1995b]. The directions of the magnetosheath magnetic fields for oscillations of *Williams* [1979] and *Lepping and Burlaga* [1979] were not specified in their observations. However, *Miura* [1995a, 1995b] showed that the magnetopause is succeptible to the K-H instability even when the magnetosheath magnetic field is not largely northward and when the magnetic tension force plays a stabilizing role. Therefore, it is reasonable to assume that the oscillations found by *Williams* [1979] and *Lepping and Burlaga* [1979] were also caused by the K-H instability. In making Figure 5 the distances along the magnetopause from the subsolar point to the location of the satellites were measured by knowing a satellite position in the GSM X-Y coordinate and by using a magnetopause model shown in Figure 11 of *Spreiter et al.* [1966]. A solid line in Figure 5 is the regression line (4), which is characterized by C=10.0 and D=61.7.

From the comparison of Figure 3 for the random initial perturbation with Figure 5 we obtain 2a= 3010km and V_0=766km/sec based on (5) and (6). From the comparison of Figure 4 for the coherent initial perturbation with Figure 5 we obtain 2a=1570km and V_0=399km/sec based on (5) and (6).

Discussion and Conclusions

An important assumption in the present inverse problem is the assumption of a constant magnetosheath flow speed V_0 along the magnetopause. Actually, however, the magnetosheath flow speed V_0 is a function of L_S and changes from zero at the subsolar point to the free streaming solar wind speed at the tail flank. If an elaborate form of the flow speed such as $V_0(L_S) = V_S L_S/(L_S + L_0)$, where V_S and L_0 are constants, is used in obtaining (3), the period τ has an extra component proportional to L_S^{-1}. A fitting of the real data based on such a functional form would require more data points in Figure 5. Therefore, we assumed for simplicity that V_0 is a constant.

By using the two extreme seed perturbations of the K-H instability, i.e., the random and the coherent seed perturbations, we obtained 2a=1570km-3010km and V_0=399km/sec-

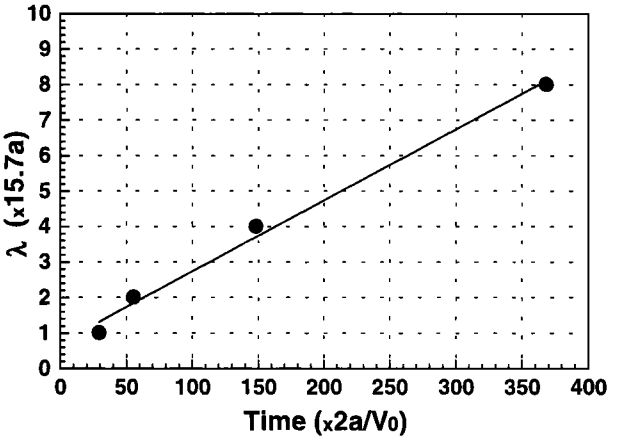

Figure 4. The wavelength of each subharmonic normalized by λ_{FGM} as a function of time t, when the subharmonic has the peak amplitude, for the simulation run with a coherent initial seed perturbation [*Miura*, 1998]. The solid line is a regression line.

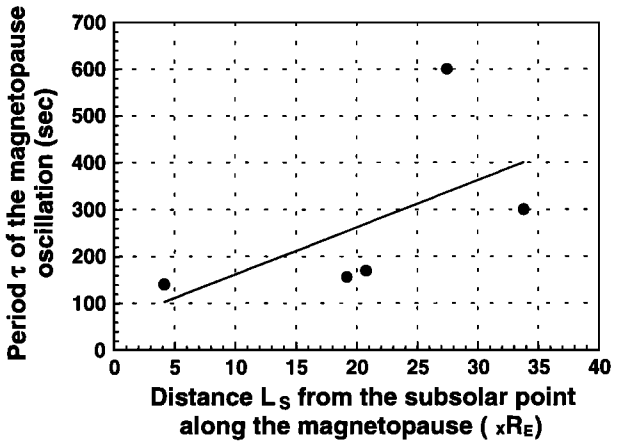

Figure 5. Observed period of the magnetopause oscillation as a function of the distance from the subsolar point to the satellite along the magnetopause. The data points from the left are due to *Williams* [1979], *Kokubun et al.* [1994], *Lepping and Burlaga* [1979], *Seon et al.* [1995], and *Chen et al.* [1993]. The solid line is a regression line.

766km/sec from the comparison of the simulation results with the observations. If a different initial seed perturbation is used, the result of the comparison will yield a thickness and an average magnetosheath flow speed between the above two extreme cases. Although the data available are limited, the comparison gives a reasonable measure of the thickness of the velocity shear layer near the subsolar point, which has never been obtained previously. This thickness is a few times larger than the typical thickness of the current layer at the magnetopause (~1000km). This variance of the two thicknesses is due to the difference of the dissipation mechanisms of the magnetic field and the flow velocity and may be important in understanding the magnetopause structure. *Eastman et al.* [1976] observed the magnetopause at low latitudes from the subsolar region back to $X=-25R_E$ and found that the magnetosheath flow velocity near the magnetopause is 300km/sec-500km/sec (see their Figure 1). This observed velocity is almost consistent with the proposed range of the average magnetosheath flow velocity obtained in the present inverse problem. If the linear relationship obtained from Figure 5 is extrapolated to a distant tail at $L_S=200R_E$, the oscillation period becomes 34min and this period falls within a range 10min-40min of the period of the magnetopause crossings observed by *Sibeck et al.* [1987] at $X=-200R_E$.

Let us hope that more data, in particular, that beyond the distance $40R_E$ from the subsolar point, will enable a more reliable test of the self-organization hypothesis and a more accurate determination of the thickness of the velocity shear layer near the subsolar point, which is so important for the theory of the magnetopause.

Acknowledgements. The author would like to thank the referees for constructive comments. This work has been supported by Grants-in-aid for Scientific Research 09640529 and, in part, by RASC of Kyoto University, ISAS and CRL as a joint research project. The computation for this work was performed at the computer center of the University of Tokyo.

References

Belmont, G., and G. Chanteur, Advances in magnetopause Kelvin-Helmholtz instability studies, *Phys. Scr.*, *40*, 124, 1989.

Chen, S.-H., M.G. Kivelson, J.T. Gosling, R.J Walker, and A.J. Lazarus, Anomalous aspects of magnetosheath flow and shape and oscillation of the magnetopause during an interval of strongly northward interplanetary magnetic field, *J Geophys. Res.*, *98*, 5727, 1993.

Eastman, T.E., E.W. Hones, Jr., S.J. Bame, and J.R Asbridge, The magnetospheric boundary layer: Site of plasma, momentum, and energy transfer from the magnetosheath into the magnetosphere, *Geophys. Res. Lett.*, *3*, 685, 1976.

Kokubun, S., H. Kawano, M. Nakamura, T. Yamamoto, K. Tsuruda, H. Hayakawa, A. Matsuoka, and L.A. Frank, Quasi-periodic oscillation of the magnetopause during northward sheath magnetic field, *Geophys. Res. Lett.*, *21*, 2883, 1994.

Lepping, R.P., and L.F. Burlaga, Geomagnetopause surface fluctuations observed by Voyager 1, *J. Geophys. Res.*, *84*, 7099, 1979.

Manuel, J.R., and J.C. Samson, The spatial development of the low latitude boundary layer, *J. Geophys. Res.*, *98*, 17367, 1993.

Miura, A., Kelvin-Helmholtz instability at the magnetopause: Computer simulations, in *Physics of the Magnetopause, Geophysical Monogr. Ser.*, vol. 90, edited by P. Song, B.U. Ö. Sonnerup, and M.F. Thomsen, p 285, AGU, Washington, D.C., 1995a.

Miura, A., Dependence of the magnetopause Kelvin-Helmholtz instability on the orientation of the magnetosheath magnetic field, *Geophys. Res. Lett.*, *22*, 2993, 1995b.

Miura, A., Compressible magnetohydrodynamic Kelvin-Helmholtz instability with vortex pairing in the two-dimensional transverse configuration, *Phys. Plasmas*, *4*, 2871, 1997.

Miura, A., Self-organization in the two-dimensional magnetohydrodynamic transverse Kelvin-Helmholtz instability, *J. Geophys. Res.*, in press, 1998.

Miura, A., and P.L. Pritchett, Nonlocal stability analysis of the MHD Kelvin-Helmholtz instability in a compressible plasma, *J. Geophys Res*, *87*, 7431, 1982.

Seon, J., L.A. Frank, A.J Lazarus, and R.P. Lepping, Surface waves on the tailward flanks of the earth's magnetopause, *J. Geophys Res*, *100*, 11907, 1995

Sibeck, D.G., J.A Slavin, and E.J Smith, ISEE 3 magnetopause crossings:Evidence for the Kelvin-Helmholtz instability, in *Magnetotail Physics*, edited by A.T.Y. Lui, p.73, Johns Hopkins University Press, Baltimore, Md. 1987.

Spreiter, J.R., A.L. Summers, and A.Y. Alksne, Hydromagnetic flow around the magnetosphere, *Planet Space Sci*, *14*, 223, 1966

Williams, D.J., Magnetopause characteristics inferred from three-dimensional energetic particle distributions, *J. Geophys. Res.*, *84*, 101, 1979.

Wu, C.C., Kelvin-Helmholtz instability at the magnetopause boundary, *J Geophys. Res*, *91*, 3042, 1986.

A. Miura, Department of Earth and Planetary Physics, University of Tokyo, Hongo 7-3-1, Bunkyo-ku, Tokyo, 113-0033, Japan. (e-mail: miura@sunepl geoph s.u-tokyo.ac jp)

(Received October 12, 1998; revised November 23, 1998, accepted November 25, 1998.)